Supplementary Information for

Massive, eco-friendly, and facile fabrication of multi-functional anodic aluminum oxides: Applications to nanoporous template and sensing platform

Seok Hwan Jeong,‡[a] Hea Lin Im,‡[a] Seongin Hong,[a] Heekyeong Park,[a] Jongyeol Baek,[a] Dong Hyuk Park,*[b] Sunkook Kim,*[a] and Young Ki Hong*[a]

[a] Department of Electronics and Radio Engineering, Kyung Hee University, Gyeonggi, 446-701, Republic of Korea.

[b] Department of Applied Organic Materials Engineering, Inha University, Incheon 402-751, Republic of Korea.

‡ These authors contributed equally to this work.

*E-mail: donghyuk@inha.ac.kr (Dong Hyuk Park), intel0616@gmail.com (Sunkook Kim), imhyke0419@gmail.com (Young Ki Hong)

(1) Experimental conditions of the AAO fabrication

Purified (99.9%) platinum cylinder (diameter × length = 2.0 mm × 50.0 mm) was purchased from Whatmann Co., and used as a counter electrode. Purified (99.99%) aluminum (Al) plates was purchased from Goodfellow Inc., and cut into a rectangular parallelepiped with width, length, and thickness of 20.0 mm, 50.0 mm, and 1.0 mm, respectively, which was used as s working electrode without thermal annealing. First, the Al substrate was ultra-sonicated in acetone for 30 min and rinsed with deionized water for removing organic residues on the multi-surfaces. The electropolishing procedure was performed by applying forward bias of +20 V in a solution of perchloric acid (60%) and absolute ethanol ($HClO_4 : C_2H_5OH = 1 : 4$, v/v) at 7 ^{o}C for about 5 min.[S1-3] The pre and main simultaneous multi-surfaces anodization (SMSA) procedures were conducted by applying anodic bias of +40.0 V in an oxalic acid aqueous solution (0.3 M).[S1,2,4,5] The temperatures (0 ^{o}C, 5 ^{o}C, 10 ^{o}C, and 15 ^{o}C) of the oxalic acid electrolytes were controlled by using double-jacket beaker, magnetic stirrer, and low-temperature bath circulator (RW-1025G, JEIO TECH). The anodic aluminum oxide (AAO) layers produced by the pre-SMSA and alumina residues after stair-like reverse biases (SRBs)-detachment were removed through chemical etching in a chromic acid aqueous solution ($H_3PO_4 : CrO_3$ = 0.56 M : 0.18 M) at ~60 ^{o}C.[S4,6,7]

(2) Syntheses of π-conjugated polymer nanowires

For removing the barrier oxide selectively as well as minimizing nanopore-widening effects, the barrier side of the AAO was floated on a sodium hydroxide aqueous solution (2.0 M) for a few seconds. Then, the pore-widening procedure was carried out by immersing the barrier-removed AAO completely into a phosphoric acid aqueous solution (1 wt%) at 50–60 ^{o}C until the nanopore diameter (D_P) reached the target values. For comparison, AAO templates with the minimum D_P of ~100 nm and ~200 nm were purchased from Whatman Co. 3-methylthiophene (3-MT, 98% purified), pyrrole (98% purified), tetrabutylammonium hexafluorophosphate ($TBAPF_6$, 96% purified one), and acetonitrile (CH_3CN) were purchased from Aldrich.

For the electrolyte used in the nanomaterials synthesis, monomers (3-MT and pyrrole) and dopants ($TBAPF_6$) were dissolved in organic solvent (CH_3CN) with monomer to dopant molar ratio of 5: 1.[S8,9] Thin gold (Au) layer was thermally evaporated on one side of the through-hole AAO with desired D_P under high vacuum conditions ($\leq 10^{-5}$ torr). The AAO with thin Au layer was attached to stainless steel plate, and immersed into the electrolyte. Then, polymer nanowires (NWs) were synthesized through a galvanostatic mode of the electrochemical polymerization method. Synthetic temperatures were maintained respectively at -40 °C for poly (3-methylthiophene) (P3MT)[S8-11] and room temperature for polypyrrole.[S8,12] After polymerization, AAO was eliminated by using hydrofluoric acid solution (2.0 M) for obtaining isolated strands of the nanomaterials.

(3) Fabrication of humidity sensors

Thin layers of Al/Au (10 nm/100 nm) were deposited on one side of the AAO with barrier oxide layer by E-beam evaporation. Then, two electrodes coupled with interdigitating structure were patterned through the conventional photolithography and lift-off techniques. The line width and distance between the adjacent lines in the electrodes were set to be ~200 μm, respectively.

(4) Characterization

The current–time (*I*–*t*) characteristic curves of the two-step SMSAs and SRBs-detachment procedures were measured by programmable DC power supply with RS-232C interfaced PC program. The AAOs, π-conjugated polymer NWs, and interdigitating electrodes on the humidity sensors were investigated using a scanning electron microscope (SEM; JSM-5200, JEOL), a transmission electron microscope (JEM-2010, JEOL), and an optical microscope

(BX51M, Olympus). Thicknesses of the AAO and Al were measured by a digital micrometer (IP65, Mitutoyo). Spatial distributions of the equipotential lines during the SMSA were obtained by a commercial electric field simulation software (ElecNet, Infolytica). The optical properties of the P3MT NWs dispersed in chloroform were characterized through ultraviolet-visible absorption spectra (HP8453, Agilent). Relative humidity (RH) were controlled through a constant temperature and humidity chamber (Enviros KCL-1000, EYELA), and capacitance variation with respect to RH were recorded by a precision LCR meter (4284A, Agilent) at 100 kHz and 1 MHz, respectively.

(5) AAOs fabricated at fixed temperature of 15 °C

Fig. S3 shows a photograph of the remaining Al substrate and AAOs produced from the every surfaces of the single Al substrate through 1_{st} to 5_{th} sequences in oxalic acid electrolyte at fixed temperature of 15 °C under standard mild anodization conditions (0.3 M, +40 V). Definition of each surfaces is same as the manuscript, which depends on the relative position with respect to the counter electrode (L: Left, R: Right, F: Front, Ba: Back, and Bo: Bottom). Yellowish-colored AAOs with equal dimensions of the corresponding surfaces were successfully obtained through the SRBs-detachment. As increasing the applied sequences, AAOs from two sides and bottom surfaces became narrower, which reflected the reduction of the total anodizing area.

Fig. S4 shows the SEM images of the open-pore sides of the AAOs detached from left (a, c, and e) and right (b, d, and f) surfaces of the same Al substrate at every odd sequences. Shape and distribution of the nanopores exhibited more complicated and less ordered natures, comparing with those in Fig. 3. These results were originated from the roughness of the two sides and bottom surfaces of the Al substrate were much poorer than front and back surface, even after electropolishing procedure.[S3] As shown in the insets of the Fig. S4, a cleavage plane through SRBs-detachment was confirmed beneath the barrier oxide layer.

(6) Dimensional analyses of the as-prepared AAOs

Dimensional characteristics, such as initial nanopore diameter (D_{P0}), interpore distance (D_{int}), and areas of nanopore/hexagonal unit cell in the AAOs, were extracted from the SEM images by using an image processing software (ImageJ, National Institute of Health). Fig. S5a shows a correlation between D_{int} and unit cell area (S). As shown in the inset of Fig. S5a, we postulated that ideal unit cells with a shape of regular hexagon are perfectly arranged into honeycomb structure without defects. The area of each unit cell was obtained from the insets of the SEM images in Fig. 3 by using ImageJ software, and converted to corresponding D_{int} through the following equations;

$$S = \frac{3\sqrt{3}}{2}a^2 \Longrightarrow D_{int} = \sqrt{3}a$$

where a is a side length of a unit cell.

Fig. S5b shows a correlation between D_{P0} and cross sectional area (A_{P0}) of the corresponding nanopore, which was postulated as an ideal circle. The area of each A_{P0} was obtained from the SEM images in Fig. 3 by using ImageJ software, and converted through the following equation;

$$A_{P0} = \pi\left(\frac{D_{P0}}{2}\right)^2$$

References

S1 H. Masuda and M. Satoh, *Jpn. J. Appl. Phys.*, 1996, **35**, L126-L129.

S2 F. Li, L. Zhang and R. M. Metzger, *Chem. Mater.*, 1998, **10**, 2470-2480.

S3 Y. K. Hong, B. H. Kim, D. I. Kim, D. H. Park and J. Joo, *RSC Adv.*, 2015, **5**, 26872-26877.

S4 A. P. Li, F. Müller, A. Bimer, K. Nielsch and U. Gösele, *J. Appl. Phys.*, 1998, **84**, 6023-6026.

S5 K. Nielsch, J. Choi, K. Schwirn, R. B. Wehrspohn and U. Gösele, *Nano Lett.*, 2002, **2**, 677-680.

S6 H. Asoh, K. Nishio, M. Nakao, T. Tamamura and H. Masuda, *J. Electrochem. Soc.*, 2001, **148**, B152-B156.

S7 H. Masuda and K. Fukuda, *Science*, 1995, **268**, 1466-1468.

S8 Y. K. Hong, D. H. Park, S. H. Lee and J. Joo, *Adv. Polym. Sci.*, 2013, **259**, 201-244.

S9 D. H. Park, M. S. Kim and J. Joo, *Chem. Soc. Rev.*, 2010, **39**, 2439-2452.

S10 Y. K. Hong, D. H. Park, S. K. Park, H. Song, D. C. Kim, J. Kim, Y. H. Han, O. K. Park, B. C. Lee and J. Joo, *Adv. Funct. Mater.*, 2009, **19**, 567-572.

S11 D. H. Park, H. S. Kim, M. Y. Jeong, Y. B. Lee, H. J. Kim, D. C. Kim, J. Kim and J. Joo, *Adv. Funct. Mater.*, 2008, **18**, 2526-2534.

S12 Y. K. Hong, D. H. Park, S. H. Park, S. K. Park and J. Joo, *Appl. Phys. Lett.*, 2009, **94**, 053111.

Table S1 Characteristic dimensions of the as-prepared AAOs shown in Fig. 3 as functions of the electrolyte temperatures and applied sequences.

Applied Sequence (*n*)	**Electrolyte Temperature (°C)**	**D_{P0} (nm)** [a]		**D_{int} (nm)** [b]		**Thickness (μm)**	
		Front	**Back**	**Front**	**Back**	**Front**	**Back**
1	0	24.5 ± 2.08	24.0 ± 2.96	97.5 ± 2.70	96.7 ± 2.24	28.8 ± 1.69	26.5 ± 1.18
2	5	31.3 ± 1.84	31.7 ± 2.06	97.6 ± 2.77	97.3 ± 1.80	48.6 ± 3.06	42.0 ± 2.54
3	10	37.3 ± 1.40	36.8 ± 2.29	97.8 ± 2.18	97.6 ± 2.01	64.9 ± 5.30	55.5 ± 2.11
4	15	44.2 ± 2.71	44.6 ± 3.61	97.7 ± 1.99	97.8 ± 2.85	82.4 ± 5.17	74.5 ± 2.17
5	15	44.9 ± 1.72	44.9 ± 2.37	98.1 ± 2.64	97.8 ± 2.36	79.7 ± 5.50	72.9 ± 1.66
6	15	45.2 ± 1.89	44.7 ± 1.88	97.8 ± 2.53	97.7 ± 1.70	83.3 ± 3.40	77.9 ± 1.52

[a] D_{P0} was calculated from the cross-sectional area of the corresponding nanopore.

[b] D_{int} was calculated from the area of the corresponding unit cell.

Table S2 Average thicknesses of the AAOs shown in Fig. 5i as functions of the Main-SMSA times at fixed electrolyte temperature of 15 °C.

Main-SMSA Time (h)		1	2	4	8	10	12	15
Thickness (μm)	**Front**	11.9 ± 1.27	20.6 ± 3.34	36.3 ± 2.21	63.7 ± 1.70	78.9 ± 3.84	96.6 ± 3.89	114.5 ± 4.28
	Back	11.4 ± 0.74	19.8 ± 1.55	32.8 ± 1.40	59.1 ± 1.45	72.9 ± 1.66	91.0 ± 3.53	109.6 ± 2.72

Table S3 Averaged D_P of the AAO shown in Fig. 5a with respect to pore-widening time in the dilute phosphoric acid solution.

Widening Time (min)	0 [a)]	5	15	25	35	45	55
D_P (nm)	24.5 ± 2.50	27.6 ± 1.48	34.9 ± 1.37	45.3 ± 1.75	52.2 ± 1.84	65.4 ± 2.56	72.9 ± 2.72

[a)] AAOs fabricated at 0 °C were chosen as starting samples for the pore-widening procedures.

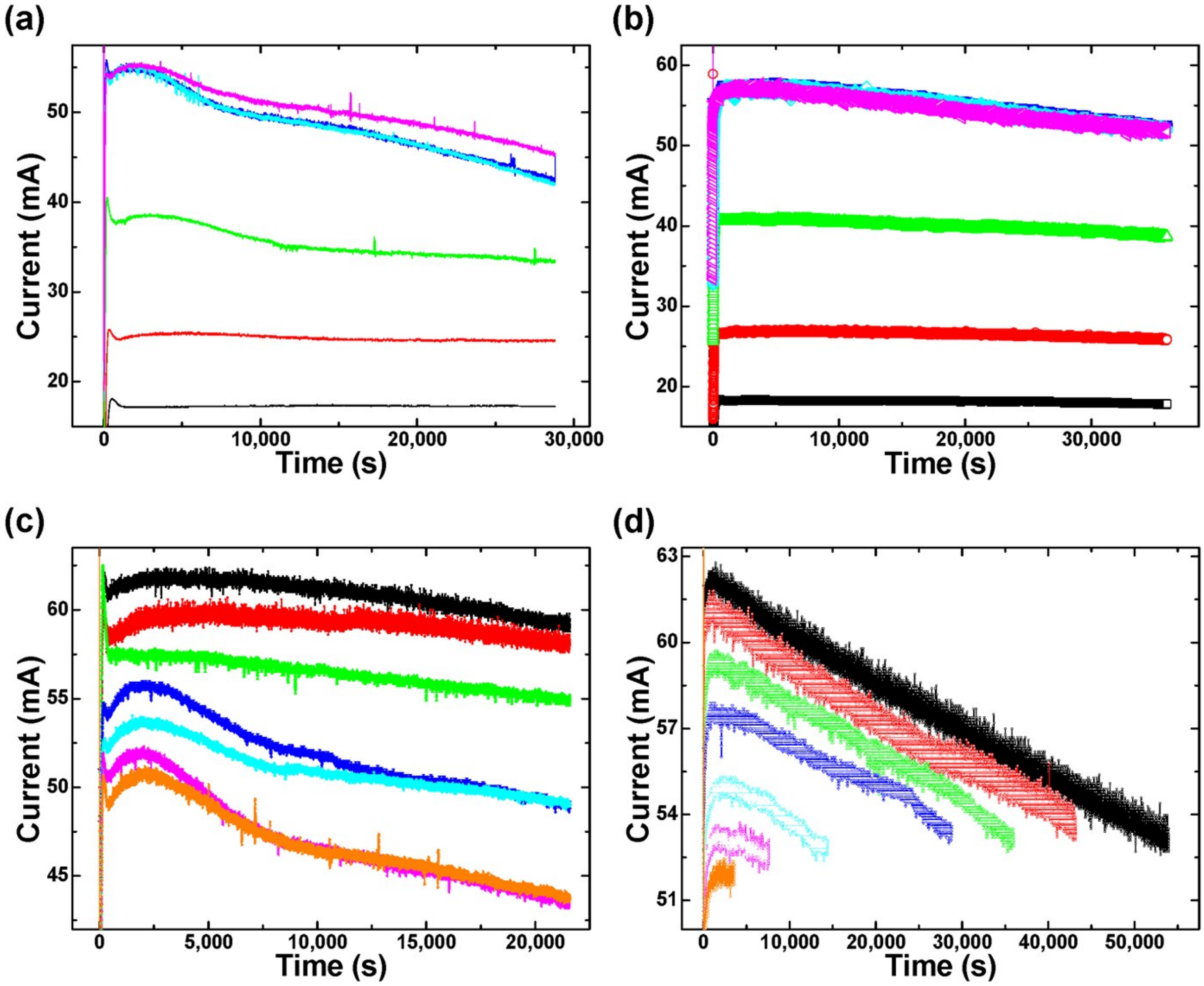
(a)
Current (mA)
20
30
40
50
0
10,000
20,000
30,000
Time (s)
(b)
Current (mA)
20
30
40
50
60
0
10,000
20,000
30,000
Time (s)
(c)
Current (mA)
45
50
55
60
0
5,000
10,000
15,000
20,000
Time (s)
(d)
Current (mA)
51
54
57
60
63
0
10,000
20,000
30,000
40,000
50,000
Time (s)

Fig. S1 Comparison of the *I*–*t* characteristic curves in linear time scale; (a, c) Pre- and (b, d) Main-SMSAs with respect to various electrolyte temperatures and anodizing times, respectively.

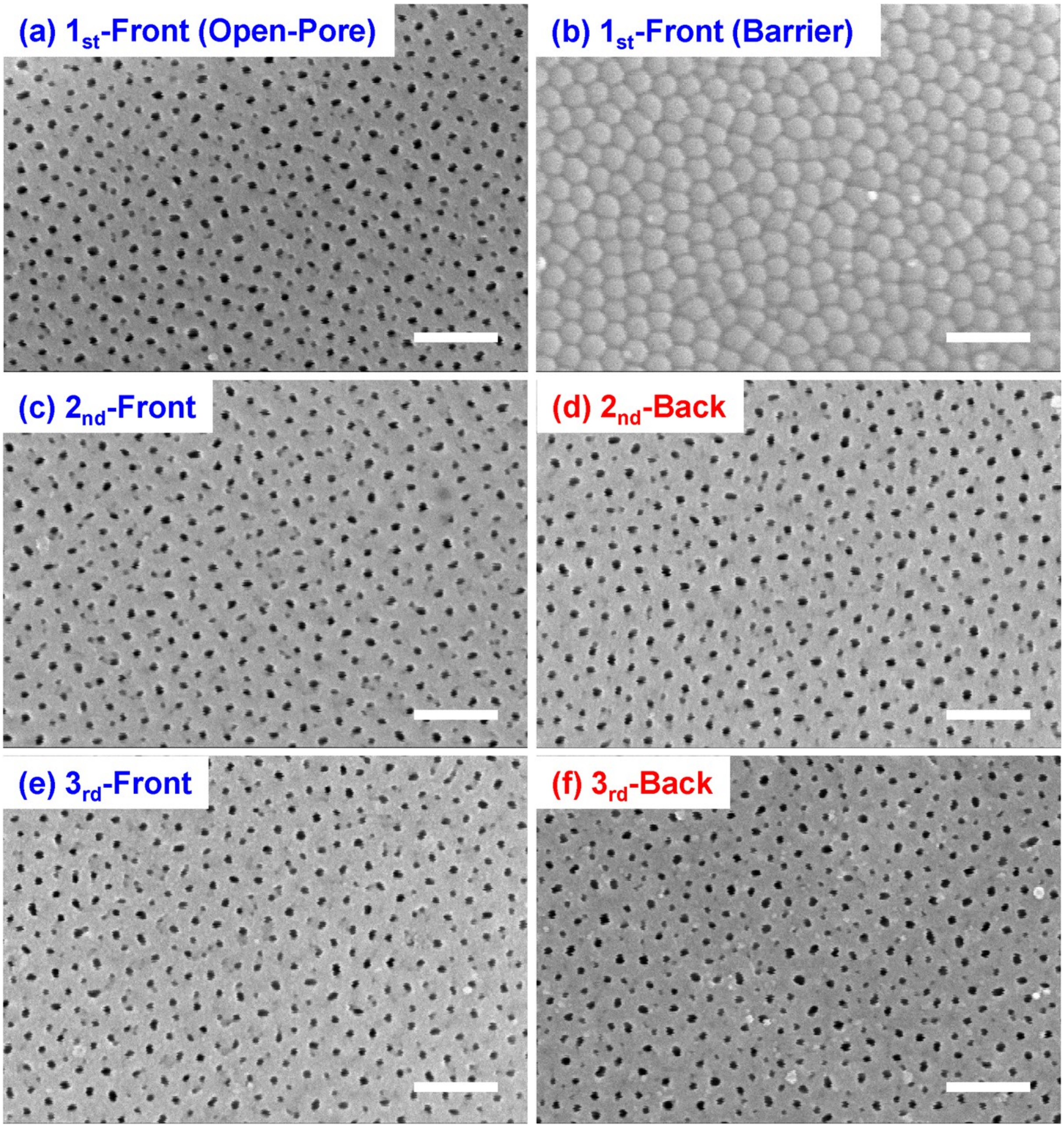

Fig. S2 SEM images of the Pre-AAOs detached through SRBs technique from front and back surfaces of the single Al substrate; (a) open-pore and (b) barrier side of 1_{st}-Front AAO, (c) 2_{nd}-Front AAO, (d) 2_{nd}-Back AAO, (e) 3_{rd}-Front AAO, and (f) 3_{rd}-Back AAO. All the scale bars are 200 nm.

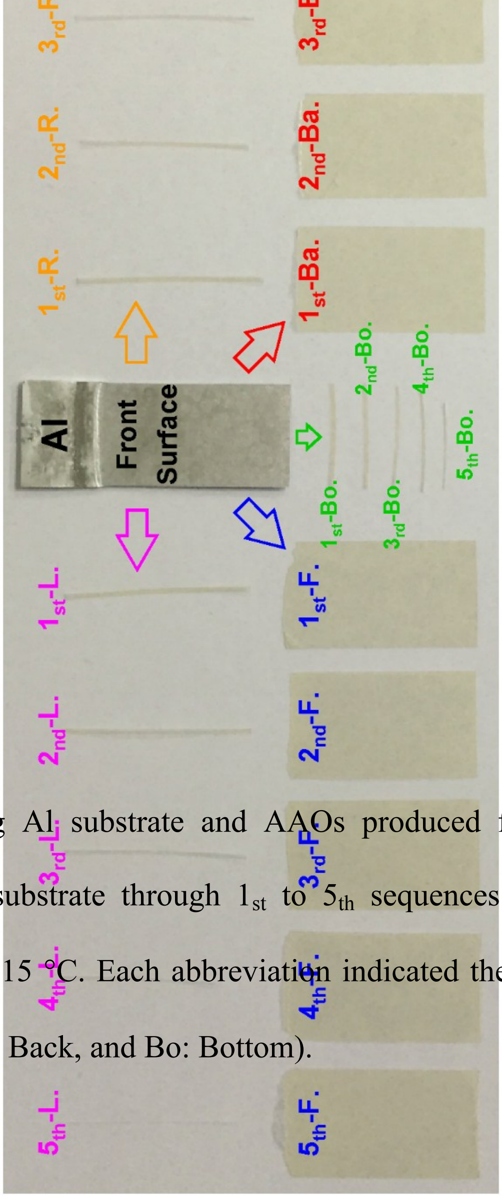

Fig. S3 Photograph of the remaining Al substrate and AAOs produced from the every immersed surfaces of the single Al substrate through 1_{st} to 5_{th} sequences in oxalic acid electrolyte under fixed temperature of 15 °C. Each abbreviation indicated the corresponding surface (L: Left, R: Right, F: Front, Ba: Back, and Bo: Bottom).

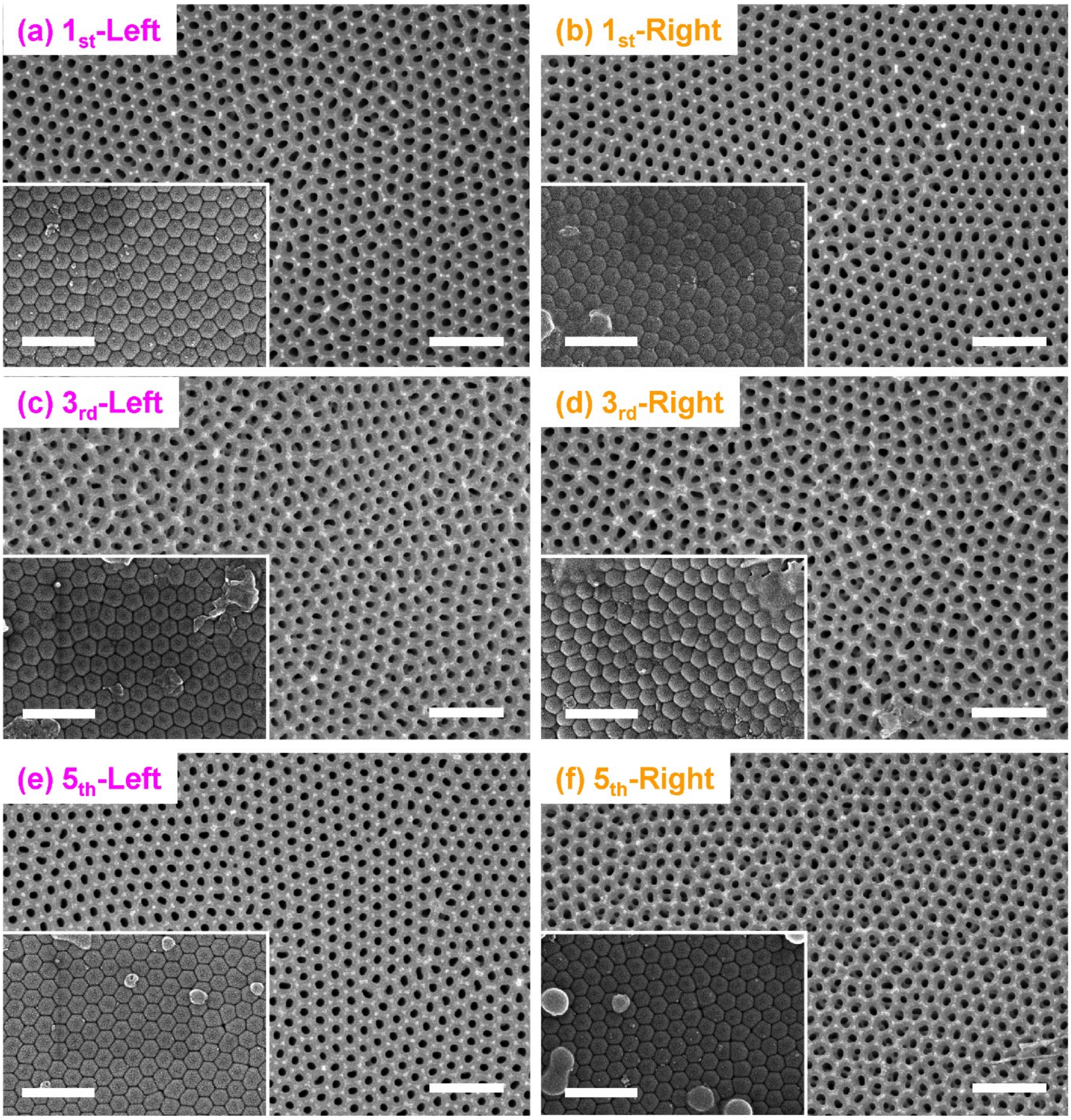

Fig. S4 SEM images of the open-pore side of the AAO produced from the both sides surfaces of the single Al substrate; (a) 1_{st}-Left AAO, (b) 1_{st}-Right AAO, (c) 3_{rd}-Left AAO, (d) 3_{rd}-Right AAO, (e) 5_{th}-Left AAO, and (f) 5_{th}-Right AAO. The insets show the SEM images of the barrier sides of the corresponding AAOs. All the scale bars are 400 nm.

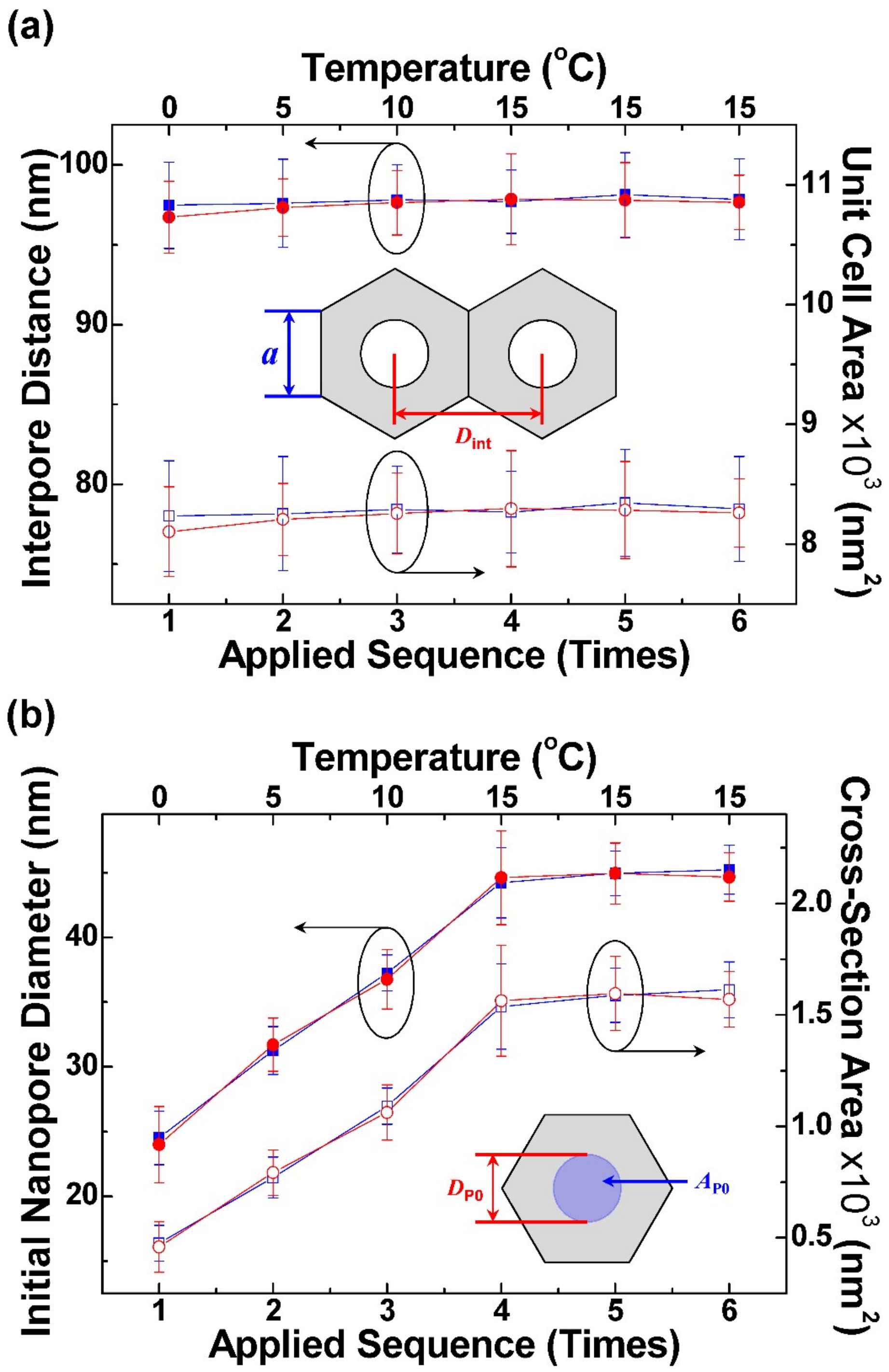

Fig. S5 Dimensional analyses of the as-prepared AAOs with respect to the electrolyte temperatures and applied sequences. (a) Correlation between interpore distance and unit cell area. The inset shows the schematic top view of the two adjacent unit cells and nanopores. (b) Correlation between initial nanopore diameter and cross sectional area of the corresponding nanopore. The inset shows the schematic top view of the single unit cell and nanopore.